Region 2
UNIVERSITY TRANSPORTATION RESEARCH CENTER

Development of Advanced Modeling Tools for Hotspot Analysis of Transportation Emissions

Prepared by

K. Max Zhang,
Sibley School of Mechanical and Aerospace Engineering
Cornell University

H. Oliver Gao
School of Civil and Environmental Engineering
Cornell University

Cornell University
School of Civil & Environmental Engineering
220 Hollister Hall
Ithaca, NY 14853
Phone: 607-254-8334
Fax: 607-255-9004
http://www.cee.cornell.edu/contact/index.cfm

July 29, 2009

Disclaimer

The contents of this report reflect the views of the authors, who are responsible for the facts and the accuracy of the information presented herein. The contents do not necessarily reflect the official views or policies of the UTRC or the Federal Highway Administration. This report does not constitute a standard, specification or regulation. This document is disseminated under the sponsorship of the Department of Transportation, University Transportation Centers Program, in the interest of information exchange. The U.S. Government assumes no liability for the contents or use thereof.

TECHNICAL REPORT STANDARD TITLE PAGE

1. Report No.	2. Government Accession No.	3. Recipient's Catalog No.

4. Title and Subtitle	5. Report Date
Development of Advanced Modeling Tools for Hotpot Analysis of Transportation Emissions	July 29, 2009.
	6. Performing Organization Code
7. Author(s)	8. Performing Organization Report No.
K. Max Zhang, Cornell University, Oliver Gao, Cornell	49777-22-19
9. Performing Organization Name and Address	10. Work Unit No.
Cornell University 220 Hollister Hall Ithaca, NY 14853	11. Contract or Grant No.
	13. Type of Report and Period Covered
12. Sponsoring Agency Name and Address	Final Report 12/31/07- 06/30/09
University Transportation Research Center City College of New York New York, NY 10031	14. Sponsoring Agency Code

15. Supplementary Notes

16. Abstract

Hot-spot analysis, also known as project-level analysis, assesses impacts of transportation emissions on local air pollution of carbon monoxide (CO), air toxics and particulate matter (PM). It is required for regional transportation plans (RTP), transportation improvement programs (TIP) and transportation project development/modification by transportation conformity rules and NEPA process. Such transportation conformity studies are particularly important in non-attainment areas and locales with concentrated and heavily traveled transportation infrastructures (e.g., major transportation corridors, border crossings, congested intersections, etc.).

Gaussian plume dispersion models of line sources such as CALINE4 have been widely used in quantitative hot-spot analysis of CO from transportation sources and have proven successful in modeling inert gaseous pollutants such as CO with sound scientific basis satisfying empirical accuracy. However, the current hotspot analysis modeling tools used by the transportation management community are not capable of simulating the air quality impact of complex roadway network in typical urban environments and not treating explicitly the various turbulent mixing processes near roadways. Those limitations hinder the accurate assessment of environmental and health impacts of transportation emissions.

In this report, we present the development of two advanced modeling tools for hotspot analysis of transportation emissions. One is a multi-link dispersion model (MLDM) based on USEPA regulatory dispersion model AERMOD. And the other is a computation fluid dynamics (CFD) model that incorporates vehicle-induced turbulence (VIT) and road-induced turbulence (RIT), named CFD-VIT-RIT. We applied the CFD-VIT-RIT model in simulating the spatial gradients of carbon monoxide near two major highways with different traffic mix and roadway configurations. The modeling results were compared to the field measurements and those from CALINE4 model, which does not account for VIT and RIT. We demonstrated that the incorporation of RIT considerably improved the modeling predictions, especially on the vertical gradients of carbon monoxide. Our study implies that roadway designs can significant influence the near-road air pollution. Thus we recommend that mitigating near-road air pollution through roadway designs be considered in the air quality and transportation management. In addition, thanks to their rigorous representation of turbulent mixing mechanisms, CFD models can become valuable tools in the roadway designs process.

17. Key Words	18. Distribution Statement
Hot-Spot, Air Pollution, Fluid Dynamics, Air Toxics, Carbon Monoxide, Roadway Designs.	

19. Security Classif (of this report)	20. Security Classif. (of this page)	21. No of Pages	22. Price
Unclassified	Unclassified	24	

Form DOT F 1700.7 (8-69)

Development of Advanced Modeling Tools for Hotpot Analysis of Transportation Emissions

Final Report to University Transportation Research Center

Principal Investigator:
K. Max Zhang, Assistant Professor
Sibley School of Mechanical and Aerospace Engineering
Cornell University
287 Grumman Hall
Ithaca, NY 14853
Tel: 607-254-5402; Fax: 607-255-1222; Email: kz33@cornell.edu

Co-Principal Investigator:
H. Oliver Gao, Assistant Professor
School of Civil and Environmental Engineering
Cornell University
325 Hollister Hall
Ithaca, NY 14853
Tel: 607-254-8334; Fax: 607-255-9004; Email: hg55@ cornell.edu

July 29, 2009

Executive Summary

Hot-spot analysis, also known as project-level analysis, assesses impacts of transportation emissions on local air pollution of carbon monoxide (CO), air toxics and particulate matter (PM). It is required for regional transportation plans (RTP), transportation improvement programs (TIP) and transportation project development/modification by transportation conformity rules and NEPA process. Such transportation conformity studies are particularly important in non-attainment areas and locales with concentrated and heavily traveled transportation infrastructures (e.g., major transportation corridors, border crossings, congested intersections, etc.).

Gaussian plume dispersion models of line sources such as CALINE4 have been widely used in quantitative hot-spot analysis of CO from transportation sources and have proven successful in modeling inert gaseous pollutants such as CO with sound scientific basis satisfying empirical accuracy. However, the current hotspot analysis modeling tools used by the transportation management community are not capable of simulating the air quality impact of complex roadway network in typical urban environments and not treating explicitly the various turbulent mixing processes near roadways. Those limitations hinder the accurate assessment of environmental and health impacts of transportation emissions.

In this report, we present the development of two advanced modeling tools for hotspot analysis of transportation emissions. One is a multi-link dispersion model (MLDM) based on USEPA regulatory dispersion model AERMOD. We applied MLDM to South Bronx, where the high childhood asthma rates have been linked to exposure to diesel particulate matters from transportation emissions. We demonstrated the capability of MLDM in simulating the spatial variations of diesel-generated particulate matter in the complex urban environment with multiple interstate highways and numerous arterial and local roads.

The other is a computation fluid dynamics (CFD) model that incorporates vehicle-induced turbulence (VIT) and road-induced turbulence (RIT), named CFD-VIT-RIT. RIT includes the turbulence generated by road embankment, road surface thermal effects and roadside structures, which are all determined by the roadway designs. We applied the CFD-VIT-RIT model in simulating the spatial gradients of carbon monoxide near two major highways with different traffic mix and roadway configurations. The modeling results were compared to the field measurements and those from CALINE4 model, which does not account for VIT and RIT. We demonstrated that the incorporation of RIT considerably improved the modeling predictions, especially on the vertical gradients of carbon monoxide. Our study implies that roadway design can significant influence the near-road air pollution. Thus we recommend that mitigating near-road air pollution through roadway designs be considered in the air quality and transportation management. In addition, thanks to their rigorous representation of turbulent mixing mechanisms, CFD models can become valuable tools in the roadway designs process.

1. Introduction

Hot-spot analysis, also known as project-level analysis, assesses impacts of transportation emissions on local air pollution of carbon monoxide (CO), air toxics and particulate matter (PM). It is required for regional transportation plans (RTP), transportation improvement programs (TIP) and transportation project development/modification by transportation conformity rules and NEPA process. Such transportation conformity studies are particularly important in non-attainment areas and locales with concentrated and heavily traveled transportation infrastructures (e.g., major transportation corridors, border crossings, congested intersections, etc.). Gaussian plume dispersion models of line sources have been widely used in quantitative hot-spot analysis of CO from transportation sources. These models incorporate the effects of dispersion caused by dilution and air movement. These models have proven successful in modeling inert gaseous pollutants such as CO with sound scientific basis satisfying empirical accuracy.

However, the Gaussian dispersion models do not account for any chemical reactions or other physical dynamics such as condensation, coagulation and deposition; which have been shown critical for quantitative modeling of particulate matter (PM) on hot-spot spatial scales. Quantitative hot-spot modeling tools are scarce to adequately characterize gradients in concentrations of PM, PM components (such as black carbon), and PM precursors near roadways. On the other hand, fast growing evidence of the adverse effects of fine particles on public health, especially of those near roadways, has pushed the imperative need for such tools that can be used in transportation planning, air quality management and exposure assessment. Cook et al. developed a methodology to resolve spatial gradient near roadways[1]. At the core of the methodology are 1) a "bottom-up" approach was employed to develop a detailed highway vehicle emission inventory that includes emissions for individual road links using travel demand models and geographical information systems software, and 2) a Gaussian dispersion model to provide texture within the modeling domain because of spatial gradients associated with highway vehicle emissions and other local sources.

In this report, we present the development of two advanced modeling tools that can be applied to hotspot analysis of transportation emissions. One is a multi-link dispersion model (MLDM) based on USEPA regulatory dispersion model AERMOD. The other is a computation fluid dynamics (CFD) model that incorporates vehicle-induced turbulence (VIT) and road-induced turbulence (RIT), named CFD-VIT-RIT.

MLDM is applied to simulate to black carbon particles near roadways in South Bronx, New York. The model is validated by the measurement data collected during a field study in 2004. CFD-VIT-RIT is applied to simulate the CO dispersion near two highways in Los Angeles, CA. The model is validated by the measurement data collected during a field study in 2002.

2. Development of a Multi-Link Dispersion Model (MLDM)

2.1 Background

The New York Metropolitan Area (NYMA) has been ranked the highest in the nation in terms of health impacts from diesel fine particles. According to a 2005 report by the Clean Air Task

Force, diesel fine particles shortened over 2,700 lives in the NYMA in 1999, more than in any of the other 39 regions studied.

Among the five boroughs of NYC, the Bronx has ranked highest in both asthma hospitalizations and deaths in recent years. Between 1990 and 2000, the asthma rates decreased only 3% in the Bronx, as compared to 39% and 35% reduction in Brooklyn and Manhattan during the same period according to New York City Department of Health and Mental Hygiene. Although the origin of asthma is unquestionably multi-factorial, recent studies have linked asthma to exposure to diesel particulate matters from transportation emissions [2, 3].

From a transportation perspective, the South Bronx has large volumes of heavy vehicle traffic passing through it along several major highways (i.e., Interstates 87, 95, 278, and 895) that encircle the South Bronx, creating pollution that can affect local residents under any wind direction. In addition, there are multiple local industries and facilities that generate truck traffic, including Hunts Point Wholesale Markets, a municipal sewage sludge processing plant, a privately owned sludge drying plant, and 19 public and private waste transfer stations. The area also hosts a municipal waste water treatment plant and a large number of manufacturing facilities. All of this traffic results in high concentrations of truck activity and diesel emissions in the proximity of schools and residences in the South Bronx. At Hunts Point Market alone, some 12,000 trucks move in and out daily according to NYSDOT.

There have been several field studies on the spatial variability, or in transportation terms "hotspots" of particulate air pollution in the South Bronx. Lena et al. measured fine particulate matter ($PM_{2.5}$) and black carbon (BC) on sidewalks and tested whether spatial variations in concentrations were related to local truck traffic density[4]. These results show that airborne EC concentrations, an important component of diesel exhaust particulates, are elevated in Hunts Point and that the impact varies across the community as a function of large truck traffic. Maciejczyk et al. employed a mobile laboratory for continuous measurements of concentrations of $PM_{2.5}$, BC, and gaseous pollutants at 6 locations for three–four weeks, each during the period of April 2001 to February 2003[5]. Overall, their sampling data indicate that the major highways encircling the South Bronx, as well as other local sources, are having a measurable adverse impact on residents' exposures to air pollution, even relative to other NYC area locales.

2.2 Dispersion Model

We chose AERMOD, developed by the American Meteorological Society/Environmental Protection Agency Regulatory Model Improvement Committee (AERMIC), as the dispersion model for MLDM. AERMOD is a modeling system incorporating air dispersion based on planetary boundary layer, turbulence structure, and scaling concepts with treatment of both surface and elevated sources, and both simple and complex terrain [6, 7]. AERMOD modeling system requires two input data processors namely AERMET and AERMAP as mandatory components. While AERMET is a meteorological data preprocessor that combines air dispersion on the basis of planetary boundary layer turbulence structure and scaling concepts, AERMAP works as a terrain data preprocessor that incorporates complex terrain though the use of USGS Digital Elevation Model Data.

2.3 Roadside Modeling Domain, Grid Resolution, And Topography

The roadside modeling domain was chosen to a 900 m by 900 m area on the east side of the South Bronx, consisting of major roads and the Harlem River dividing Manhattan Island and Bronx, with grid resolution of 6 m x 6 m. Figure 1 illustrate the modeling domain using the Universal Transverse Mercator map projection zone 18 (UTM18) with the map centered at x = +590,206 m and y = +4,518,871 m, which is the location of roadside monitoring. Topography of the study area was obtained from the U.S. Geological Survey (USGS) Digital Elevation Model (DEM). We used 7.5-minute DEM data with 10-m resolution to acquire the elevations of the emission sources and receptors.

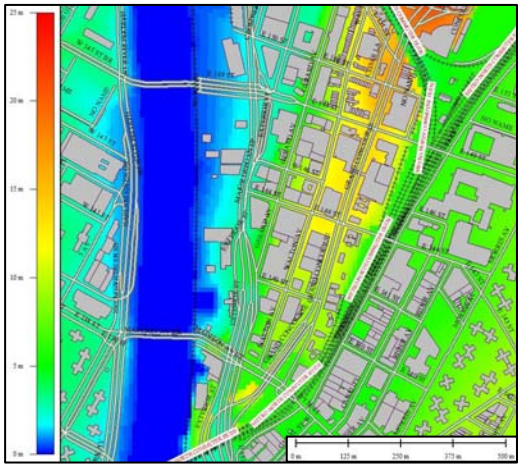

Figure 1. Roadside modeling domain with buildings footprint, transportation line, and terrain elevation

2.4 Meteorological Data

Observational meteorological data used in this study consist of on-site, surface, and upper air data. On-site data were directly measured inside the roadside modeling domain including temperature, relative humidity, wind direction, and wind speed [8]. Surface and upper air data were obtained from the nearest National Weather Service (NWS) monitoring stations, which routinely report meteorological parameters such as temperature, dew point, wind direction, wind speed, cloud cover, cloud layer(s), ceiling height, visibility, current weather, and precipitation amount at surface level. The nearest surface air NWS station is located in the Central Park, New York City, and the nearest upper air NWS station is located at Brookhaven, NY. Using integrated onsite, surface, and upper air can eliminate uncertainties in model calculation.

2.5 Microscale Emission Inventory

The data for creating the link-level road network were acquired from the New York Metropolitan Transportation Council (NYMTC)'s Best Practice Model (BPM). The BPM is a travel demand forecasting model consisting of a package of analytical procedures that include simulation of the region's highway and transit system, a land use/development model, and post processing proce-

dures for predicting the air quality impacts of region transportation programs. The software TransCAD was used to run the Best Practice Model.

The traffic activities on the road links were obtained from two sources, the real-time traffic video recorded during the roadside monitoring and NYMTC's BPM. The traffic video was analyzed to yield the traffic volume, speed and vehicle distribution on the section of I-87 near the roadside monitoring location. The traffic activities for the rest of the road links were obtained from the BPM, which divide each day into four time segments, i.e., early morning, mid day, afternoon, and evening.

The primary vehicle emission factor model in the U.S. is MOBILE 6, developed by USEPA Office of Transportation and Air Quality. New York State Department of Transportation (NYSDOT) modified the USEPA Mobile6 model to reflect the vehicle conditions in New York, which is recommended for air quality analyses for NYSDOT programs and projects. Thus we adopted the MOBILE6.2 emission factor tables provided by NYSDOT to derive the PM2.5 emission factors of different vehicle types. BC emission factors are not directly available from either USEPA or NYSDOT. The relative fractions of BC in PM2.5 emissions from mobile sources were obtained from SPECIATE (Version 4.0), USEPA's repository of total organic compound (TOC) and particulate matter (PM) speciation profiles of air pollution sources.

All point emissions were extracted from the 2002 National Emission Inventory (NEI). The speciation profiles for those sources were acquired from SPECIATE.

The current AERMOD model is not capable of simulating line sources directly. To overcome this barrier, we divided the road links into multiple segments. Each segment was then modeled as an area source with its length-to-width ratio smaller than 10, consistent with the definition of area sources in AERMOD. Figure 4 depicts the roadway segments to represent the road links specified in NYMTC's BPM.

2.6 Roadside Monitoring Of Black Carbon

A detailed description of the roadside monitoring study was documented by Patel et al [8]. A brief description is presented here. The field measurements were conducted from in an urban school, referred as U2, in South Bronx from February to March 2004. U2 is located 34 meters east of a major highway with annual average daily traffic of 85,000 vehicles.

BC was monitored using a dual-beam aethalometer (Model AE-21, Magee Scientific, Berkeley CA). A weather station (Vantage Pro Model 6150C, Davis Instrument Corp., Hayward, CA) was installed on each school roof to monitor and record temperature, relative humidity, barometric pressure, wind speed and direction, and precipitation. The weather station is equipped with data logger and computer software interface (WeatherLink, Davis Instrument Corp., Hayward, CA) for storing, downloading and processing meteorological data, which were downloaded once a week. Traffic data were collected using two different methods: a real time traffic counter and video camera. Real-time traffic data were collected using Trax RD Automatic Traffic Recorder (Jamar Technologies Inc, Horsham, PA), which collects traffic data from tubes that are laid across the roadway.

2.7 Model Evaluation

We compared the predicted BC concentrations by MLDM against the measured values on 8 days (March 12 to 18, and March 20 to 22, 2004) during the sampling period, when all instruments functioned normally from 6 am to 4 pm daily and no precipitation occurred. Figure 2 illustrates the results.

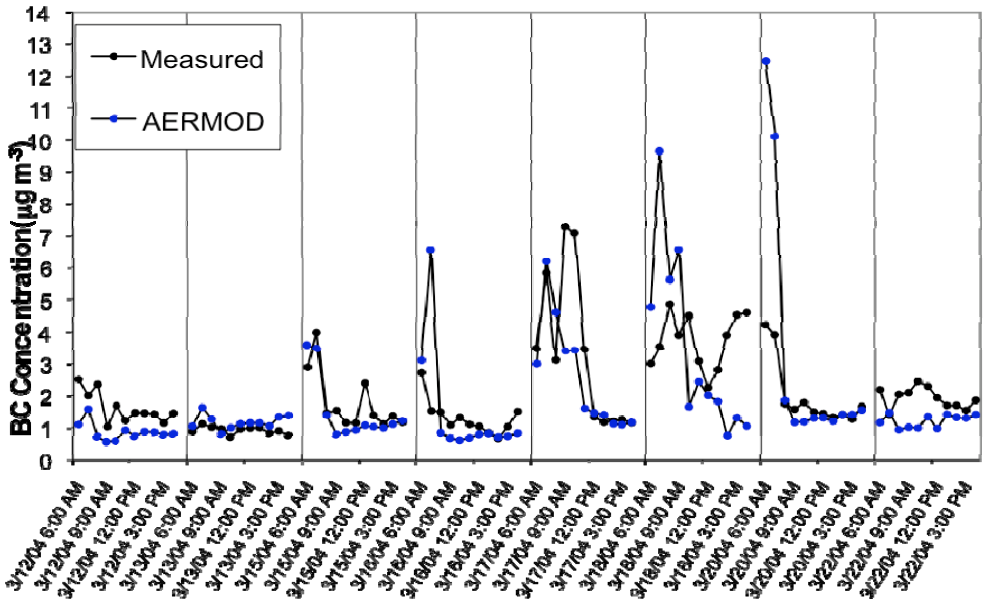

Figure 2. Time series plot of measured and predicted black carbon concentrations at U2.

Next, we evaluated the MLDM model performance using statistical metrics. Among the reported performance metrics being used for air quality model performance assessment, there are five main statistical measures to evaluate the dispersion model in terms of operational performance to determine its degree of acceptability and applicability of the specific task (Yu et al., 2006), namely Mean Normalized Error (MNE), Mean Normalized Bias (MNB), Unpaired Peak Accuracy (UPA), Mean Fraction Error (MFE) and Mean Fraction Bias (MFB). Those statistical measures are formulated in Table 1.

Table 1. Statistic measures formulations

Statistical Measures	Formulas	Ranges
Mean Normalized Error (MNE)	$MNE = \frac{1}{N}\sum_{i=1}^{N}\left\lvert\frac{Model_i - Obs_i}{Obs_i}\right\rvert \times 100\%$	0 to +∞ %
Mean Normalized Bias (MNB)	$MNB = \frac{1}{N}\sum_{i=1}^{N}\left(\frac{Model_i - Obs_i}{Obs_i}\right) \times 100\%$	-100 to +∞ %

Unpaired Peak Accuracy (UPA)	$UPA = \frac{Model_{MAX} - Obs_{MAX}}{Obs_{MAX}} \times 100\%$	-100 to +∞ %
Mean Fraction Error (MFE)	$MFE = \frac{1}{N}\sum_{i-1}^{N} \frac{\lvert Model_i - Obs_i \rvert}{(Model_i + Obs_i / 2)} \times 100\%$	0 to +200%
Mean Fraction Bias (MFB)	$MFB = \frac{1}{N}\sum_{i-1}^{N} \frac{(Model_i - Obs_i)}{(Model_i + Obs_i / 2)} \times 100\%$	-200 to +200%

**N is the number of estimate-observation pairs down from all data from station i for the comparison time period of interest, $Model_i$ is the model-estimated concentration at station i, Obs_i is the observed concentration at station i*

We applied the MLDM modeling results and the measurement data to calculate those metrics for our simulations listed in Table 2.

Table 2. MLDM model evaluation results

Statistical Measures	***AERMOD***	***Accepted Criteria***
Mean Normalized Error (MNE)	+40%	+30 to +35% [i]
Mean Normalized Bias (MNB)	-6%	±5 to ±15% [i]
Unpaired Peak Accuracy (UPA)	+71%	±15 to ±20% [i]
Mean Fraction Error (MFE)	+26%	≤ ±75% [ii]
Mean Fraction Bias (MFB)	-10%	≤ ±60% [ii]

Source: [i] [9, 10]

For the statistical measures based on relative difference between model prediction and observation values including MNE and MNB, the results of AERMOD (MNE = 40%, MNB = -6%) were considered acceptable. However, the UPA value (71%) was far beyond the acceptance criteria.

The underlying assumptions for using metrics such as MNE, MNB and UPA is that the observation data are considered entirely correct. Nevertheless, uncertainties in instruments and traffic analysis may have contributed to the observed discrepancies between the predicted and measurement values. The alternative metrics MFE and MFB, which do not assume that the observations are absolute accurate, are considered more appropriate to judge model acceptability and perform performance [10, 11]. Based on MFE and MFB values, AEROMOD predictions (MFE = 26%, MFB = -10%) were considered to be satisfactory.

2.8 Spatial Variation of Black Carbon in South Bronx

Once validated, MLDM was applied to simulate the spatial variations of BC in South Bronx. The simulation domain was a 6 km by 6 km area encompassing highways and arterial roads. As described earlier, the road links were divided to road segments to be modeled as area sources. Due to the large number of road links in the domain, we created over 6,000 road segments for our

simulation as shown in Figure 3(a). The emissions from the mobile and stationary sources were estimated in the same method discussed earlier.

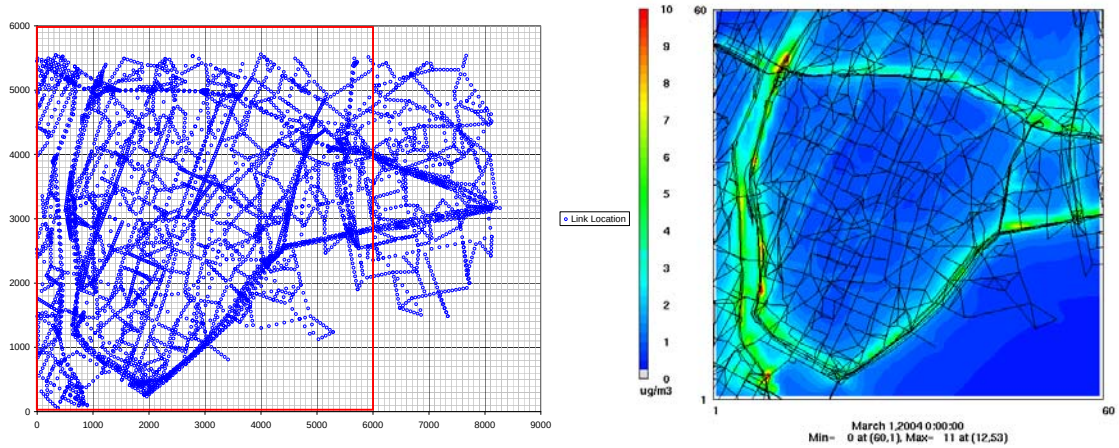

Figure 3. Simulation of spatial variations of black carbon (BC) concentrations in South Bronx. (a) Modeled (over 6,000) road segments. (b) 24-hour average BC concentration in South Bronx on March 18, 2004

Figure 3(b) depicts an example of contour plots representing the spatial variations of BC concentrations in South Bronx.

This paper presented a viable approach for simulating BC spatial variation. However, more detailed information is needed to fully describe the BC concentrations in the region. NYMTC's BPM does not include local roads. The NYC Metro is the most populated urban conglomeration area across the United States, with approximately fifteen million people eating food distributed through the Hunts Point food center (e.g., facilities like the produce market, the fish center, and the meat market) daily. Truck traffic induced by the food facilities starts entering the Hunts Point neighborhood hours before sunrise under expressways or over highways, accumulating more than 15,000 trucks by sunset. These trucks, virtually all powered by diesel fuel, keep gunning emissions of diesel toxicants as they rattle down any routes deemed efficient by the drivers (including slipping down side streets passing residential neighborhood) in the often congested stop-and-go traffic, of which trucks are only a fraction of the more than 77,000 vehicles travelling through the South Bronx (The City of New York, PlaNYC).

3. Development of CFD-VIT-RIT model

3.1 Background

In Section 3, we aim to investigate the effects of different turbulent mixing mechanisms on pollution dispersion near roadways. In recent years, computational fluid dynamics (CFD) have been applied in modeling the dynamical and mechanical processes taking place in complicated urban environments such as street canyons and road tunnels However, CFD models have not been applied to simulate near-road air quality in an open highway environment and the effects of different turbulent mixing mechanisms have not been thoroughly examined.

Highway dispersion is caused by turbulent mixing on-road and near-road. Several mechanisms can affect the generation of turbulence near roadways in addition to atmospheric boundary layer turbulence (*ABLT*). Firstly, the movement of vehicles on the road results in a significant increase in turbulence [12, 13]. Secondly, turbulence can be generated by the embankment on which a highway was located when wind flew over it [14]. Thirdly, thermal effects caused by solar radiation generate turbulence during hot season and cannot be ignored for pollutant dispersion [15-17]. Fourthly, road structures (i.e., noise barrier, tree planting) can also produce turbulence that influences the flow field [18-20]. In contrast to the turbulence by moving vehicles (often called vehicles-induced turbulence, or *VIT*), the last three types of turbulences described above can all be attributed to roadways designs, which are referred to as road-induced turbulence (*RIT*).

An improved CFD model with detailed treatment of VIT and RIT was used to simulate the horizontal and vertical dispersions of CO in the vicinity of two highways during two seasons. This model is referred to as CFD-VIT-RIT. This paper is organized as follows. First, we introduce the different mixing mechanisms and their characteristics. Then, the field measurement that provided the data used to validate the CFD-VIT-RIT model is briefly described. Next, the configuration of the CFD-VIT-RIT model is discussed. The modeling results are presented in two categories, one on the contributions of different mixing mechanisms to the total kinetic energy on and near roadway, and the other comparing the horizontal and vertical gradients of CO from the CFD-VIT-RIT model and CALINE4. This paper is concluded with a discussion on the implications of our findings on future road design and the advantages and disadvantages of applying different dispersion models in simulating near-road air quality.

3.2 Mechanisms for VIT and RIT generation

In this section, we provide a brief summary of the mechanisms that generate VIT and RIT in the on-road and near-road environments.

Turbulence induced by vehicles. Traffic has a dominant effect in the immediate vicinity of the highway [13]. Moving vehicles enhance mixing processes by inducing turbulence, which originates from the interaction between moving vehicles and ambient air. It is known that up to 50% of kinetic energy is converted into additional turbulence when a fluid hits an obstacle [21]. The wakes behind moving vehicles are characterized as momentum wakes and contain organized trailing vortices which play a key role in determining the flux of kinetic energy and rapidly mix the pollutants released in the turbulent wake [13, 22, 23]. The vehicle-induced turbulence, which is strongly related to vehicle type and speed [24-27], can be expected to significantly influence the diffusion of highway emissions, especially in the microenvironment near roadways [12, 13, 24]

Turbulence induced by the embankment. The embankment acts as a topographic obstacle which causes a form drag and produces turbulence to compensate for the deformation of the flow field when wind flows over it [28]. A recirculation cavity is created downwind of the embankment, containing a well-mixed, and often lower, zone of pollution concentrations [29]. The induced turbulence depends on the wind velocity, wind direction, the height and the shape of the embankment [14, 24, 28, 29]. A field measurement was conducted on an embankment along the

Rhine River in Germany, which is elevated approximately 2.7 m above the surrounding terrain, and the non-negligible turbulence was found in the vicinity of the embankment [14].

Turbulence induced by thermal effects on road surface. The available solar radiation on a surface, Q_0, can be divided into turbulent fluxes of sensible heat, H_0, latent heat, V_0, and the soil heat flux, B_0, as $Q_0 = V_0+H_0+B_0$ [26].

With high absorptivity and low heat capacity, the asphalted surface of highway receives much net energy. Compared to the grassy or concrete surroundings, it provides a very small latent heat flux and leads to an increased sensible heat flux, which generates turbulence. The thermally induced flow is combined with mechanically induced flows, and affects the transport of pollutants. The sensible heat flux of asphalted surface was considered in the measurement in Heidelberg, Germany. The results showed a thermally generated turbulence, which contributed to about 10% of total road produced turbulence [26].

It should be noted that due to the large solar zenith angle in the winter, the road surface receives much less direct solar radiation, so the temperature difference between road surface and air can be neglected.

Turbulence induced by roadside structures. Roadside structures (i.e., noise barrier, tree planting) affect pollutant concentrations around the structure by blocking initial dispersion, and increasing turbulence and initial mixing of the emitted pollutants [18-20]. Noise barrier disturbs wind field as a still obstacle while tree planting consist of branches and leaves can be considered as a porous body [18, 20]. Field experiments and simulation results of the Quick Urban & Industrial Complex (QUIC) model showed that the plume behind noise barriers and vegetation was relatively uniform and vertically well-mixed, and pollutant concentrations were reduced under certain meteorological conditions. With winds directionally from the road, concentrations of CO and PM number generally decreased between 15 and 50% behind the noise barrier [20].

Most of the dispersion models, ranging from simple line source Gaussian plume models to elaborate numerical models in two and three dimensions, do not explicitly include the turbulence generated by moving vehicles with changing vehicle speed and type, the embankment according to the real shape and the thermal effects determined by different road structures [13, 30-32]. CFD models are capable of simulating VIT and RIT efficiently [15, 17, 21, 25, 33-37]. We incorporated the detailed representations of VIT and RIT and ABLT into a CFD model to elucidate their effects on on-road and near-road dispersion and compare the modeling results against field measurement data.

3.3 Field measurements

The experimental data utilized in this paper were collected from previous measurements near highways I-405 and I-710 in Los Angeles in the summer and winter [38-42].

I-405 is 30 m wide, with an embankment of 4.5 m-height, while I-710 is 26 m wide at ground level. The horizontal sampling points for I-405 and I-710 were taken at 30, 60, 90, 150, 300 m and 17, 30, 90, 150, 300 m downwind, respectively, and 300m upwind at height 1.6 m. Both

sampling lines were perpendicular to the corresponding highways and the distance to each sampling point was measured from the center of the highway. In addition, the vertical CO concentrations were measured at 0.6, 3.0, 5.5, 8.0, 10.4, 12.8, 15.3, and 17.7 m above the ground at a fixed location about 50 m downwind from the center of I-405 in the summer. The meteorological and road data are listed in Table 3. The detailed description of the sampling sites can be found in previous papers [38-42].

From Table 3, it is clear that, in terms of meteorological parameters, there are relatively large differences in temperature and relative humidity, but small difference in wind speed between the summer and the winter. In addition, vehicle volume for each highway showed little variations. For I-405, gasoline cars dominated the vehicle mix, while for I-710, more than 25% of the vehicles are heavy-duty diesel trucks.

Table 3 Meteorological Parameters and Road Conditions Collected during Field Experiment

Parameters	I-405		I-710	
	summer	winter	summer	winter
Temperature (°C)	30.3	23.2	30.3	23.2
Relative humidity (%)	66.4	43.1	66.4	43.1
Solar zenith angles (°)[50]	25.1	64.4	25.1	64.4
Wind velocity (m s^{-1})	1.5	1.4	1.3	1.2
Wind direction to highways (°)	90	90	90	90
Wind deviation (°)	23	23	45	45
Stability class	unstable	neutral	unstable	neutral
Traffic volume (vehicles min^{-1})	231	236	203	200
Heavy-duty truck percentage	5-6%	5-6%	25-30%	25-30%
Upwind CO concentration (ppm)	0.1	0.2	0.1	0.2

3.4 CFD-VIT-RIT model

The $k-\varepsilon$ model available in the commercial computational fluid dynamics code, FLUENT 6.3.26 version (www.fluent.com), was used for modeling flow and dispersion in the vicinity of highways and is described in the Supporting Information.

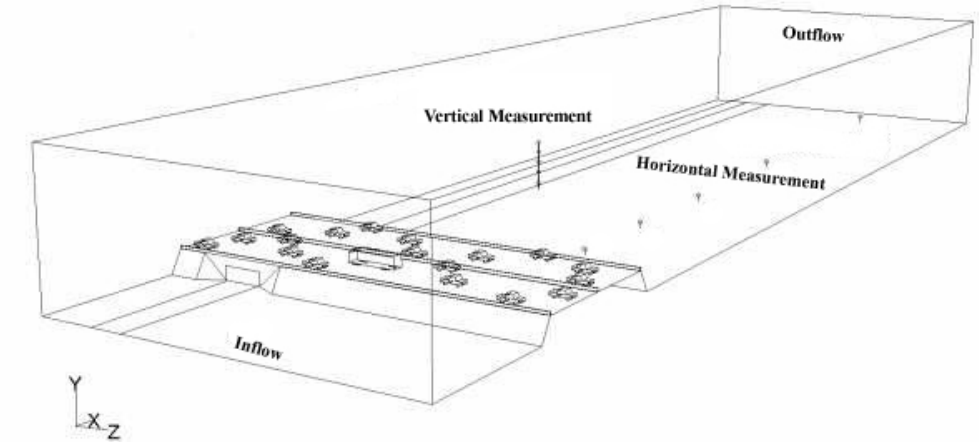

Figure 4. Geometric features of the computational domain for I-405

Figure 4 shows the three-dimensional computational domain of I-405 and the sketch of measurement locations. The number of computational cells used for the simulation was 2,305,712, with a size of 380 m by 80 m in the horizontal and 30 m in the vertical direction. The computational domain for I-710 was similar, except that the highway is not located on an embankment. The spatial domain has a size of 380 m by 40 m in the horizontal and 30 m in the vertical direction and was divided into 1,063,541 unstructured cells.

A test zone right above road surface was created to obtain the average turbulent kinetic energy (TKE). Different heights of the domain were set according to the heavy-duty truck percentage. Since most of the vehicles were cars and vans for I-405, the height of the zone is 2.5 m, while for I-710, the height is 3.5 m since it is a major truck route with about 25% of vehicles being heavy-duty truck.

We modeled the vehicles as real-shaped rather than block-shaped to keep the conditions similar to the streamlined shape of real vehicles [25], since the turbulence for the block-shaped vehicle is estimated to be 25% higher than for the true vehicle models [43]. Different types of vehicles were built approximately following their actual sizes. The measured average vehicle speed [38], was adopted for all vehicles in the simulation [44]. For the vehicle surface, an equivalent roughness height of 0.0015 m was chosen to match the simulated drag force of vehicles with the value based on drag coefficient [45]. The sketch of vehicles for I-710 is illustrated in Figure 5. Since the traffic volumes and types did not change significantly between seasons, just one set of vehicles were built for each highway.

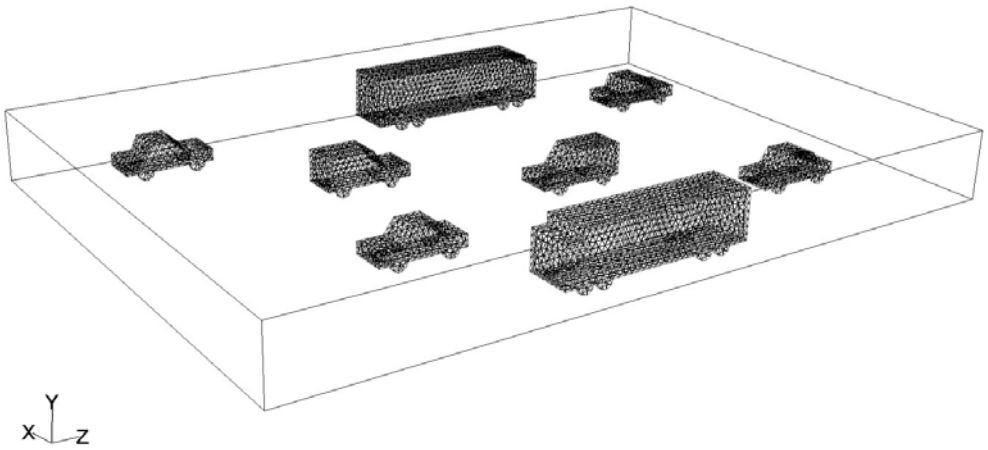

FIGURE 5. Sketch of three-dimension elements for I-710.

The embankment for I-405 was built corresponding to its real size (in Figure 1). All the solid boundaries, including ground surfaces and vehicle surfaces, are specified as non-slip boundary conditions in the flow module and are prescribed at a fixed temperature in the heat transfer module. Based on a meteorological study in Los Angeles [46], the temperature difference between air and highway surface was estimated to be 20°C for the summer season under strong solar radiation. As discussed earlier, the road surface thermal effects were neglected for both highways in the winter season.

In summary, we incorporated the turbulences induced by atmospheric wind, moving traffic, embankment and road surface thermal effects into our CFD model. Since there are no noise barriers and few trees in the surrounding of I-405 and I-710, turbulence generated by the road barriers was not studied. Considering the atmospheric wind in two seasons, wall functions were used to simulate the fully developed vertical profile of inlet wind flow [47], and are described in the Supporting Information.

3.5 Modeling Results

TKE Results. Induced TKE within the test zone is summarized in Table 4. From Table 4, it is clear that the total TKE changes with seasons and highways and that the largest TKE is obtained from I-405 with the embankment in the summer. The VIT, especially for I-710, is dominated over the boundary layer turbulence generated by the atmospheric wind, as suggested by previous wind tunnel studies [48]. Due to the large percentage of heavy-duty trucks, the VIT of I-710 is much larger than that of I-405. Similar agreements were found between the VIT's predicted by our model (0.36 $m^2 s^{-2}$ for I-405 and 0.63 $m^2 s^{-2}$ for I-710) and the empirical formula (0.37 $m^2 s^{-2}$ for I-405 and 0.64 $m^2 s^{-2}$ for I-710) reported by Baumer et al. [24]. The TKE produced by embankment is about 0.30 $m^2 s^{-2}$, which is also in good agreement with the value, 0.34 $m^2 s^{-2}$, calculated from another empirical formula in Baumer et al. [24]. Furthermore, TKE caused by the thermal effects due to road surface properties accounts for more than 18% of total TKE and therefore cannot be ignored.

Table 4. Summary of TKE

		I-405				I-710			
		summer	percentage	winter	percentage	summer	percentage	winter	percentage
Vehicle-induced TKE[a]		0.36	41.4%	0.35	53.9%	0.63	76.8%	0.63	95.5%
Road-induced TKE[a]	Embankment	0.30	34.5%	0.27	41.5%	N/A	N/A	N/A	N/A
	Road surface thermal effects	0.17	19.5%	N/A	N/A	0.15	18.3%	N/A	N/A
Atmospheric Boundary layer TKE[a]		0.04	4.6%	0.03	4.6%	0.04	4.9%	0.03	4.5%
Total TKE[a]		0.87	100%	0.65	100%	0.82	100%	0.66	100%

[a]Unit is $m^2 s^{-2}$

It should be noted that the main advantage of our model over the empirical formula is its capability to resolve the effects of VIT and RIT over the near-road region beyond the test zone. Our simulations show that TKE reaches the maximum value on road, and decays with the increasing distance from the highway, until at 300 m it is negligibly small. Due to a large turbulence dissipation rate, VIT drops below 50% at about 20 m downwind of highway. When wind velocity increases, VIT dissipates faster but is also transported to a greater horizontal distance. When wind velocity is small, VIT can spread to higher elevation. RIT decreases slower than VIT, due to the big size of the embankment which results in a larger influence range. For I-405, the ratio of VIT to RIT decreases with the increasing distance.

Spatial gradients of carbon monoxide concentrations. Results for CO dispersion in horizontal and vertical directions are compared against the field measurement data and the results from CALINE4 model [38-42], which does not account for the effects of VIT and RIT. We use

405S, 405W, 710S and 710W to refer to the studies of two different highways at two different seasons with "S" and "W" representing summer and winter, respectively.

Horizontal gradients and seasonal variations. Figure 6(a) presents the simulation results obtained from CFD-VIT-RIT model and CALINE4 against the experimental data for I-405 in the summer. CO concentration decays exponentially when moving away from the traffic source. The dilution between 30 m and 60 m vary with different models: CALINE4 underpredicts up to 33% compared to measurement data. Including VIT and RIT, the CFD model reduces the error to less than 15%. In Figure 6(b), since turbulence induced by the road surface thermal effects can be ignored in the winter, the differences in CALINE4 and CFD-VIT-RIT predictions are small. The simulation results for I-710 in the summer and winter are shown in Figure 6(c) and Figure 6(d). The improvement of predictions by CFD-VIT-RIT over CALINE4 on I-710 simulations can be attributed to the detailed treatment of VIT in CFD-VIT-RIT.

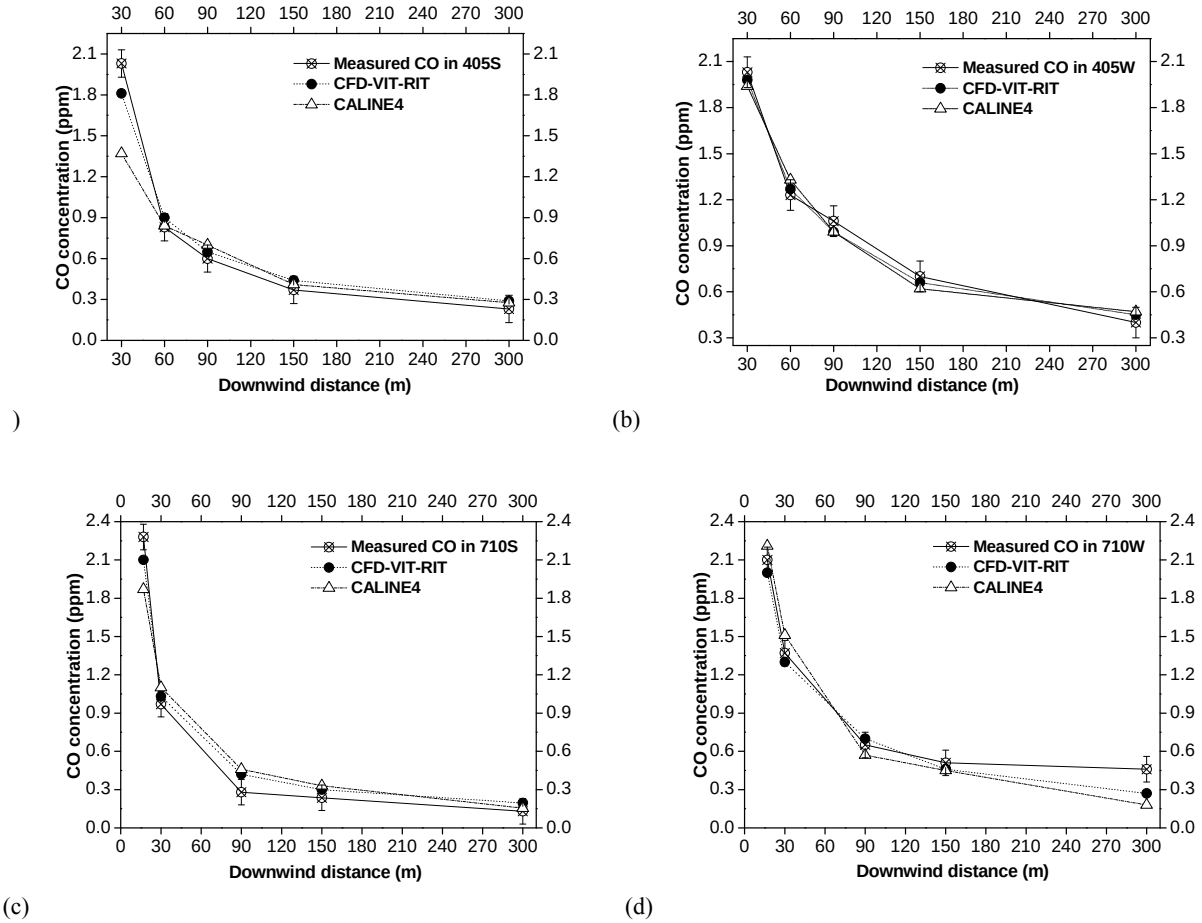

FIGURE 6. Comparison between models and field experiment for I-405 in summer (a) and winter (b); and for I-710 in summer (c) and winter (d).

The root mean square (RMS) differences between modeled and measured CO concentrations are summarized in Table 5, where the RMS of CFD model is consistently smaller than that of CALINE4 in each situation.

TABLE 5. RMS between Modeled and Measured CO Concentrations

	CFD model RMS	CALINE4 RMS
I-405 summer horizontal	0.13	0.21
I-405 winter horizontal	0.06	0.07
I-710 summer horizontal	0.14	0.26
I-710 winter horizontal	0.11	0.25
I-405 summer vertical	0.06	0.19

The horizontal dispersion of CO is determined mainly by wind velocity and turbulence [40]. To compare dispersions between 30 m and 150 m for both I-405 and I-710 in different seasons, a parameter called dilution ratio is used. More details can be found in Zhang et al. [39].

TABLE 6. Downwind CO Dilution Ratios between 30 m and 150 m

	I-405			I-710		
	summer	winter	summer/winter	summer	winter	summer/winter
Measured CO	5.08	2.9	1.75	4.11	2.69	1.53
CFD with RIT	4.11	3.01	1.37	3.53	2.95	1.20
CALINE4	3.34	3.12	1.07	3.51	3.35	1.04

From Table 6, it is clear that due to the turbulence induced by the thermal effects, dilution ratios in the summer are much larger than those of winter for both I-405 and I-710. Seasonal effects are significant with winters generally less dynamic than summers, therefore thermal effects cannot be neglected during the summer, especially under low wind conditions and wind perpendicular to the street [15, 34, 35, 39]. Meanwhile, mainly due to the existence of the embankment, dilution ratios of I-405 are higher than that of I-710 for both summer and winter. The dilution ratios obtained from CFD-VIT-RIT model show the same trend as the measurement data while CALINE4 shows little change between different seasons.

Vertical gradients. At first, the simulated wind velocity vertical profile is verified by field measurement. From Figure 7 it can be seen that measured wind velocities are approximately constant with vertical height and have relatively small and similar standard deviations [40]. CFD model shows good consistence, except at height 0.6 m, where the simulated velocity is not within the standard deviation of the measured data. The possible reason is that since the sampling point is close to the surface, it is probably disturbed by the unconsidered structure on the ground.

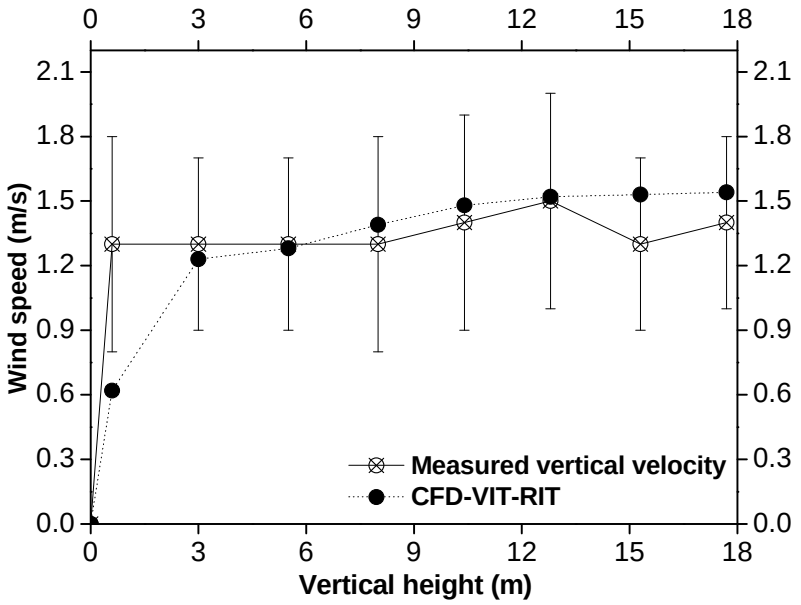

FIGURE 7. Comparison of wind velocity changing with vertical heights at 50m downwind between CFD model and field experiment for I-405 in summer. Error bars indicate one standard deviation of the measurement.

Next, Figure 8 compares the measured and simulated vertical profile of CO concentrations at 8 sampling locations from 0.6 to 18 m above the ground, and 50 m downwind of I-405 horizontally in the summer. The vertical CO concentration was observed to reach a maximum at a height around 5 m above the ground, and decrease by 30% at 18 m above the ground. There is a dimple observed at 10 m, which is likely due to a secondary mixing above the central line of emission [40]. The CFD-VIT-RIT model demonstrated great superiority in predicting CO vertical profiles compared to CALINE4. The RMS of CFD-VIT-RIT model (shown in Table 3) is only about one third of that by CALINE4. Both VIT and RIT played more significant roles in the vertical dispersion, where turbulence dominates the mixing process, than in the horizontal dispersion, where both turbulence and axial transport govern the mixing process. CFD-VIT-RIT model yields good predictions at almost all sampling points. Its maximum concentration is obtained at 6.4 m, about 1.9 m above the highway. The small rise of the plume from the highway is mainly due to the buoyancy of the exhaust induced by a higher temperature on surface of asphalted road. However, because of the strong mechanical mixing due to moving vehicles on road, the buoyant plume rise is small [13]. The simulated CO concentration at the height of 0.6 m fits measurement data well, though simulated wind velocity shows an error. This is mainly because vertical dispersion is mostly controlled by turbulence rather than wind velocity.

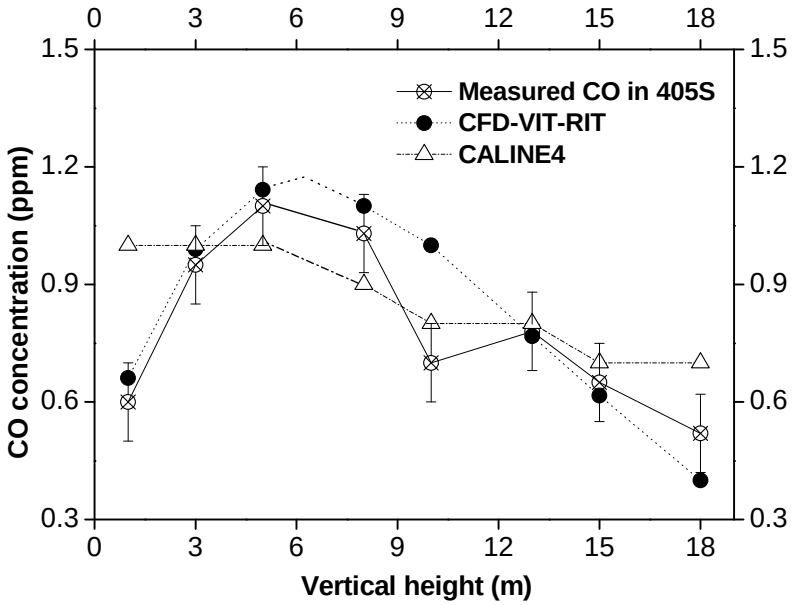

FIGURE 8. Comparison of vertical CO concentration between models and field experiment for I-405 in the summer.

3.6 Implications on Roadway Designs

We have demonstrated that the significant improvement in predicting the spatial gradients of air pollutants near roadways can be achieved by incorporating detailed treatment of vehicle-induced turbulence (VIT) and road-induced turbulence (RIT) into dispersion modeling. While VIT is governed by the traffic mix on the roadways, RIT is determined by the roadway design characteristics such as roadway configurations (e.g., elevated or depressed), road surface properties (asphalt or concrete) and roadside structures (e.g., noise and vegetation barriers). Given the large effects of RIT on pollutant dispersion, we argue that roadway designs considerably affect near-road air quality and that future roadway designs could serve as an effective strategy to mitigating near-road air pollution. Project-level analyses, known as "hot spot analyses," are required for certain transportation projects that are either funded or approved by the Federal Highway Administration (FHWA) or Federal Transit Administration (FTA). Therefore we recommend that effects of the roadway designs be taken into consideration for project-level analyses.

Nevertheless, further understanding of the effects of the roadway designs on pollution dispersion is needed before making scientifically sound policies. We are hoping that our study can initiate future investigations into this subject. CFD-VIT-RIT model is still more computationally expensive than Gaussian plume models such as CALINE4, but it is able to provide much more physical insights thanks to its rigorous treatment of turbulence mixing mechanisms on- and near-road. Moreover, the advantage of CFD-VIT-RIT is clearly shown in predicting vertical gradients of air pollutants near roadways, which is important in studying human exposure to near-road air pollution for people living at different elevations. Thus CFD-VIT-RIT, or a combination of CFD-VIT-

RIT and Gaussian plume models, could become a valuable tool in roadway design process and near-roadway air quality research.

References

1. Cook, R., et al., *Resolving local-scale emissions for modeling air quality near roadways.* Journal of the Air & Waste Management Association, 2008. **58**(3): p. 451-461.
2. Thurston, G., et al., *A study of traffic-related pm exposures and health effects among South Bronx children with asthma.* Epidemiology, 2004. **15**(4): p. S64-S64.
3. Spira-Cohen, A., et al., *A health effects analysis of traffic-related PM pollution among children with asthma in the South Bronx, NY.* Epidemiology, 2006. **17**(6): p. S229-S229.
4. Lena, T.S., et al., *Elemental carbon and PM2.5 levels in an urban community heavily impacted by truck traffic.* Environmental Health Perspectives, 2002. **110**(10): p. 1009-1015.
5. Maciejczyk, P.B., et al., *Ambient pollutant concentrations measured by a mobile laboratory in South Bronx, NY.* Atmospheric Environment, 2004. **38**(31): p. 5283-5294.
6. Perry, S.G., et al., *AERMOD: A dispersion model for industrial source applications. Part II: Model performance against 17 field study databases.* Journal of Applied Meteorology, 2005. **44**(5): p. 694-708.
7. Cimorelli, A.J., et al., *AERMOD: A dispersion model for industrial source applications. Part I: General model formulation and boundary layer characterization.* Journal of Applied Meteorology, 2005. **44**(5): p. 682-693.
8. Patel, M., *Respiratory health effects associated with exposure to traffic-related particulate matter*, in *Mailman School of Public Health*. 2007, Columbia University: New York.
9. Seinfeld, J.H. and S.N. Pandis, *Atmospheric Chemistry and Physics: From Air Pollution to Climate Change*. 2nd ed. 2006: Wiley-Interscience.
10. Boylan, J.W. and A.G. Russell, *PM and light extinction model performance metrics, goals, and criteria for three-dimensional air quality models.* Atmospheric Environment, 2006. **40**(26): p. 4946-4959.
11. Yu, S., et al., *New unbiased symmetric metrics for evaluation of air quality models.* Atmospheric Science Letters, 2006. **7**(1): p. 26-34.
12. Chock, D.P., *General-Motors sulfate dispersion experiment - An analysis of the wind-field near a road* Boundary-Layer Meteorology, 1980. **18**(4): p. 431-451.
13. Rao, K.S., et al., *Turbulence and dispersion modeling near highways.* Atmospheric Environment, 2002. **36**(27): p. 4337-4346.
14. Hauf, T. and G. Neumannhauf, *The turbulent wind flow over an embankment.* Boundary-Layer Meteorology, 1982. **24**(3): p. 357-369.
15. Kim, J.-J. and J.-J. Baik, *Urban street-canyon flows with bottom heating.* Atmospheric Environment, 2001. **35**(20): p. 3395-3404.
16. Sini, J.F., S. Anquetin, and P.G. Mestayer, *Pollutant dispersion and thermal effects in urban street canyons.* Atmospheric Environment, 1996. **30**(15): p. 2659-2677.
17. Xie, X.M., et al., *The impact of solar radiation and street layout on pollutant dispersion in street canyon.* Building and Environment, 2005. **40**(2): p. 201-212.

18. Gromke, C., et al., *Dispersion study in a street canyon with tree planting by means of wind tunnel and numerical investigations - Evaluation of CFD data with experimental data.* Atmospheric Environment, 2008. **42**(37): p. 8640-8650.
19. Lidman, J.K., *Effect of a noise wall on snow accumulation and air quality* Transportation Research Record 1985. **1033**: p. 79-88.
20. Baldauf, R., et al., *Impacts of noise barriers on near-road air quality.* Atmospheric Environment, 2008. **42**(32): p. 7502-7507.
21. Katolicky, J. and M. Jicha, *Eulerian-Lagrangian model for traffic dynamics and its impact on operational ventilation of road tunnels.* Journal of Wind Engineering and Industrial Aerodynamics, 2005. **93**(1): p. 61-77.
22. Ozdemir, E. and I.B. Ozdemir, *Turbulent structure of three-dimensional flow behind a model car: 2. Exposed to crosswind.* Journal of Turbulence, 2004. **5**: p. 18.
23. Kozaka, E.O., G. Ozkan, and I.B. Ozdemir, *Turbulent structure of three-dimensional flow behind a model car: 1. Exposed to uniform approach flow.* Journal of Turbulence, 2004. **5**: p. 22.
24. Baumer, D., B. Vogel, and F. Fiedler, *A new parameterisation of motorway-induced turbulence and its application in a numerical model.* Atmospheric Environment, 2005. **39**(31): p. 5750-5759.
25. Sahlodin, A.M., R. Sotudeh-Gharebagh, and Y.F. Zhu, *Modeling of dispersion near roadways based on the vehicle-induced turbulence concept.* Atmospheric Environment, 2007. **41**(1): p. 92-102.
26. Kalthoff, N., et al., *Vehicle-induced turbulence near a motorway.* Atmospheric Environment, 2005. **39**(31): p. 5737-5749.
27. Gronskei, K.E., *The influence of car speed on dispersion of exhaust gases.* Atmospheric Environment, 1988. **22**(2): p. 273-281.
28. Garbrecht, T., et al., *Influence of a sea ice ridge on low-level airflow.* Journal of Geophysical Research-Atmospheres, 1999. **104**(D20): p. 24499-24507.
29. Kim, H.G. and V.C. Patel, *Test of turbulence models for wind flow over terrain with separation and recirculation.* Boundary-Layer Meteorology, 2000. **94**(1): p. 5-21.
30. Benson, P.E., *A review of the development and application of the CALINE3 and CALINE4 models* Atmospheric Environment Part B-Urban Atmosphere, 1992. **26**(3): p. 379-390.
31. Coe, D.L., et al., *User's Guide for CL4: A User Friendly Interface for the CALINE4 Model for Transportation Project Impact Assessments.* Caltrans-U.C. Davis Air Quality Project, Sacamento, 1998.
32. Held, T., D.P.Y. Chang, and D.A. Niemeier, *UCD 2001: an improved model to simulate pollutant dispersion from roadways.* Atmospheric Environment, 2003. **37**(38): p. 5325-5336.
33. Yassin, M.F., R. Kellnerova, and Z. Janour, *Impact of street intersections on air quality in an urban environment.* Atmospheric Environment, 2008. **42**(20): p. 4948-4963.
34. Xie, X.M., et al., *Characteristics of air exchange in a street canyon with ground heating.* Atmospheric Environment, 2006. **40**(33): p. 6396-6409.
35. Xie, X., C.-H. Liu, and D.Y.C. Leung, *Impact of building facades and ground heating on wind flow and pollutant transport in street canyons.* Atmospheric Environment, 2007. **41**(39): p. 9030-9049.

36. Liu, C.S. and G. Ahmadi, *Computer simulation of pollutant transport and deposition near Peace Bridge.* Particulate Science and Technology, 2005. **23**(2): p. 109-127.
37. Gokhale, S. and M. Khare, *Vehicle wake factor for heterogeneous traffic in urban environments.* International Journal of Environment and Pollution, 2007. **30**(1): p. 97-105.
38. Zhang, K.M., et al., *Evolution of particle number distribution near roadways. Part III: Traffic analysis and on-road size resolved particulate emission factors.* Atmospheric Environment, 2005. **39**(22): p. 4155-4166.
39. Zhang, K.M., et al., *Evolution of particle number distribution near roadways. Part II: the 'road-to-ambient' process.* Atmospheric Environment, 2004. **38**(38): p. 6655-6665.
40. Zhu, Y.F. and W.C. Hinds, *Predicting particle number concentrations near a highway based on vertical concentration profile.* Atmospheric Environment, 2005. **39**(8): p. 1557-1566.
41. Zhu, Y.F., et al., *Study of ultrafine particles near a major highway with heavy-duty diesel traffic.* Atmospheric Environment, 2002. **36**(27): p. 4323-4335.
42. Zhu, Y.F., et al., *Seasonal trends of concentration and size distribution of ultrafine particles near major highways in Los Angeles.* Aerosol Science and Technology, 2004. **38**: p. 5-13.
43. Thompson, R.S. and R.E. Eskridge, *Turbulent diffusion behind vehicles: Experimentally determined influence of vortex pair in vehicle wake.* Atmospheric Environment (1967), 1987. **21**(10): p. 2091-2097.
44. Gidhagen, L., et al., *Model simulations of NOx and ultrafine particles close to a Swedish highway.* Environmental Science & Technology, 2004. **38**(24): p. 6730-6740.
45. White, F.M., *Fluid Mechanics.* McGraw-Hill Science Engineering, 2002.
46. Terjung, W.H. and P.A. Orourke, *The effects of changing solar angles, cloud regimes, and air temperatures on the temperatures of contrasting surfaces.* Boundary-Layer Meteorology, 1982. **24**(3): p. 269-279.
47. Blocken, B., T. Stathopoulos, and J. Carmeliet, *CFD simulation of the atmospheric boundary layer: wall function problems.* Atmospheric Environment, 2007. **41**(2): p. 238-252.
48. Khare, M., et al., *Effects of the homogeneous traffic on vertical dispersion parameter in the near field of roadways - A wind tunnel study.* Environmental Modeling & Assessment, 2005. **10**(1): p. 55-62.